Fermi National Accelerator Laboratory

FERMILAB-Conf-97/406

From Symmetry Violation to Dynamics: The Charm Window

Jeffrey A. Appel

Fermi National Accelerator Laboratory
P.O. Box 500, Batavia, Illinois 60510

December 1997

Published Proceedings of the *International Conference on Physics Since Parity Symmetry Breaking - Conference in Memory of Prof. C.S. Wu*, Nanjing, China, August 16-18, 1997

Operated by Universities Research Association Inc. under Contract No. DE-AC02-76CH03000 with the United States Department of Energy

Disclaimer

Distribution

FROM SYMMETRY VIOLATION TO DYNAMICS: THE CHARM WINDOW

JEFFREY A. APPEL
Fermilab, PO Box 500, Batavia, IL 60510 USA
E-mail: appel@fnal.gov

C.S. Wu observed parity violation in the low energy process of nuclear decay. She was the first to observe this symmetry violation anywhere. Yet, her work taught us about the form and strengths of the couplings of the massive weak boson. Today, we use the same approach. We look for very much higher mass-scale interactions through symmetry violations in the decays of charm quark systems. These charm decays provide a unique window to new physics.

1 Introduction

The Standard Model of particle physics is widely hailed for its many successes in summarizing experimental results. It is used to guide our thinking about what accelerators to build and what experiments to pursue. However, there are some very important questions which the Standard Model does not address. How is electroweak symmetry broken? Why are there three generations of quarks and leptons? Why is there such a stong matter-antimatter asymmetry in the universe? These are examples of questions whose importance is manifest, yet whose answers appear to lie beyond the purview of the Standard Model.

Many physicists believe that the answers to the above questions and others may lie at mass scales beyond those that can be reached today. One approach is to build ever more energetic accelerators in pursuit of these mass scales. Another is to look at precision measurements and at rare/forbidden processes where very high mass scales can be probed through the contributions of virtual states. This paper focuses on the latter approach, examining the unique window of opportunity in charm decay. Symmetry violations due to dynamics may be seen in searches for CP violation, particle-antiparticle mixing, and rare/forbidden decays. In each of these areas, there is a gap between current measurements and where Standard Model effects could mask new physics.

It is appropriate to consider the breaking of symmetries in otherwise rare/forbidden processes as we meet in memory of C.S. Wu and celebrate her contributions to physics. Her discovery of parity violation is an excellent example of apparently forbidden interactions giving insight into fundamental processes at a much higher mass scale. After all, it is the existence of two couplings by the massive W boson which is responsible for the low energy cobalt-decay parity violation observed in Wu's famous experiment.

1.1 Uniqueness of Charm as a Window for New Physics

Among the ways to search for evidence of new physics, we will look at one particular window of opportunity, charm decay. It is a window in the sense that there are orders of magnitude between the current limits on rates for several symmetry violating modes and the level where Standard Model effects are expected (Table 1). Within this window, there is sensitivity to a range of extensions to the Standard Model - nearly the whole gamut of proposed extensions - from Higgs to supersymmetry to technicolor and other effects.[19]

The charm quark is the only quark with charge plus 2/3 that is both unstable and yet survives long enough to bind with other quarks and form observable particles. Thus the charm quark provides a unique way to discover effects that occur only in the up-quark sector – effects that might never be observed by studying the down, strange, and bottom quarks, which all have a charge of minus 1/3.

Many effects are predicted by the Standard Model for the down-quark sector and are sought there. These effects are predicted to be small or negligible in the charm quark case. Therefore, non-Standard Model effects can show themselves in charm without being masked, an advantage that may not exist for the down-quark sector. Thus, the charm quark is potentially the only route to some kinds of physics beyond the Standard Model.

1.2 Exponential Growth of Sensitivity in Charm Physics

The sensitivity to new physics in experiments depends on the number of decays observed for a given branching rate, and the cleanliness of the signal. The first measurements were dominated by experiments at e^+e^- colliders. However, the last twenty years have seen an exponential growth in the numbers of reconstructed charm in fixed target experiments at Fermilab, and a corresponding improvement of signal to noise (Figure 1). The growth has been a factor of 100 per ten years, i.e., typically a factor of ten for each new cycle of experiment. The most prodigious sample of observed charm particles in a single experiment so far contains over 200,000 reconstructed charm decays in the most copiously reconstructed, fully-charged decay modes. The highest sensitivity measurements in charm decay now come from the Fermilab fixed target program. Experiments just completing their data taking at Fermilab should reach one million reconstructed decays.

Table 1: Window to new physics in charm decay.

Topic	90% CL Limit	ref	Std. Model prediction	ref	Typical NS Models
Direct CP Violation					
$D^0 \to K^-\pi^+$	-0.009<a<0.027	1	≈ 0 (CFD)		SUSY,
$D^0 \to K^-\pi^+\pi^-\pi^+$			≈ 0 (CFD)		LR Sym.,
$D^0 \to K^+\pi^-$			≈ 0 (DCSD)		Extra
$D^+ \to K^+\pi^+\pi^-$			≈ 0 (DCSD)		Higgs
$D^0 \to K^-K^+$	-0.093<a<0.073	2			
	-0.028<a<0.166	1			
$D^0 \to \pi^+\pi^-$	-0.186<a<0.088	2			
$D^+ \to K^-K^+\pi^+$	-0.062<a<0.034	3			
$D^+ \to \overline{K}^{*0}K^+$	-0.092<a<0.072	3	$(2.8\pm0.8) \times 10^{-3}$	5	
$D^+ \to \phi\pi^+$	-0.075<a<0.21	4			
$D^+ \to \pi^+\pi^+\pi^-$	-0.086<a<0.052	3			
$D^+ \to \eta\pi^+$			$(-1.5\pm0.4) \times 10^{-3}$	5	
$D^+ \to K_S\pi^+$	few$\times 10^{-4}$		3.3×10^{-3}	6	
FCNC					
$D^0 \to \mu^+\mu^-$	4×10^{-6}	7,8	$< 3 \times 10^{-15}$	9	4^{th} Gen.,
$D^0 \to \pi^0\mu^+\mu^-$	1.7×10^{-4}	10			Tree-level
$D^0 \to \overline{K}^0 e^+e^-$	17.0×10^{-4}	11	$< 2 \times 10^{-15}$	9	FCNC
$D^0 \to \overline{K}^0\mu^+\mu^-$	2.5×10^{-4}	10	$< 2 \times 10^{-15}$	9	
$D^+ \to \pi^+e^+e^-$	6.6×10^{-5}	12	$< 10^{-8}$	9	
$D^+ \to \pi^+\mu^+\mu^-$	1.8×10^{-5}	12	$< 10^{-8}$	9	
$D^+ \to K^+e^+e^-$	2.0×10^{-4}	13	$< 10^{-15}$	9	
$D^+ \to K^+\mu^+\mu^-$	9.7×10^{-5}	13	$< 10^{-15}$	9	
$D \to X_u + \gamma$			$\sim 10^{-5}$	9	
$D^0 \to \rho^0\gamma$	1.4×10^{-4}	9	$(1-5) \times 10^{-6}$	9	
$D^0 \to \phi\gamma$	2×10^{-4}	9	$(0.1-3.4) \times 10^{-5}$	9	
LF or LN Violation					
$D^0 \to \mu^\pm e^\mp$	1.0×10^{-4}	14	0		LQ
$D^+ \to \pi^+\mu^\pm e^\mp$	1.3×10^{-4}	13	0		
$D^+ \to K^+\mu^\pm e^\mp$	1.2×10^{-4}	13	0		
$D^+ \to \pi^-\mu^+\mu^+$	8.7×10^{-5}	13	0		
$D^+ \to K^-\mu^+\mu^+$	1.2×10^{-4}	13	0		
$D^+ \to \rho^-\mu^+\mu^+$	5.8×10^{-4}	10	0		
Mixing					
$\overset{(-)}{D}{}^0 \to K^\mp\pi^\pm$	$r < 0.0037$	15			LQ, SUSY,
	$\Delta M_D <$ 1.3×10^{-4} eV	15	10^{-7} eV	17	4^{th} Gen., Higgs
$\overset{(-)}{D}{}^0 \to K\ell\nu$	$r < 0.005$	18			

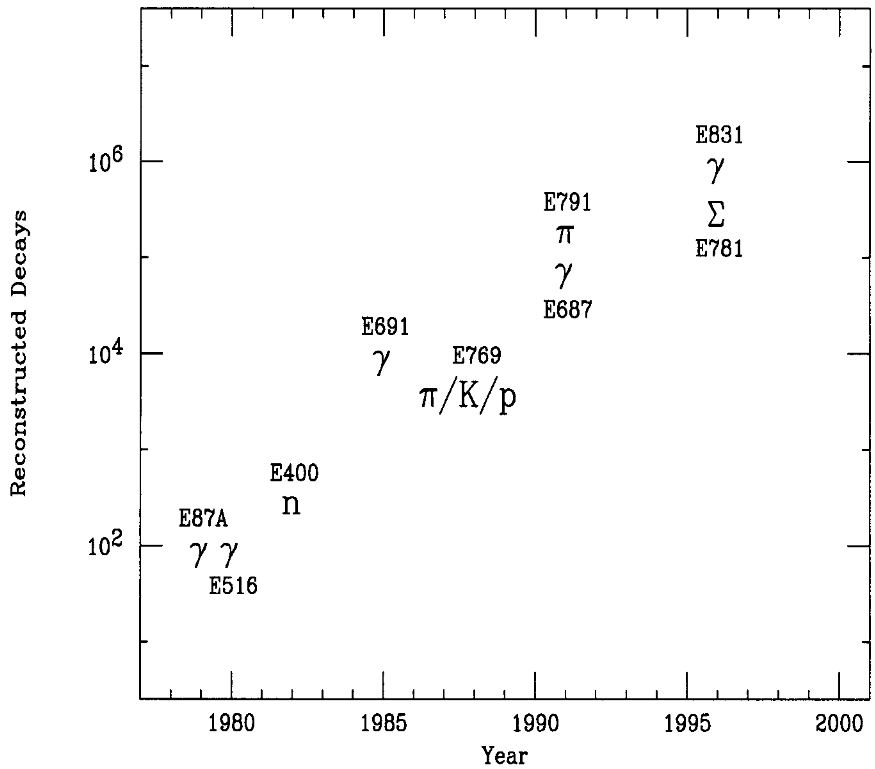

Figure 1: Exponential growth in the numbers of reconstructed charm in fixed target experiments at Fermilab. The symbols represent the beam particle types, positioned at the number of reconstructed charm decays and the year the data were taken.

Table 2: Exponential growth of charm sensitivity and data acquisition parallelism in the series of four experiments at Fermilab's Tagged Photon Laboratory; the first two experiments with γ beams, the second two experiments with secondary, charged hadron beams.

Time Frame	Exp. #	# Data Streams	# CPUs	# Output Streams	# Events on Tape $\times 10^6$	Data Set Size - GBy	# Recon. Charm
1980-2	E516	1	1	1	17	50	100
1984-5	E691	2	1	1	100	400	10,000
1987-8	E769	7	17	3	400	1500	4,000
1991-2	E791	8	54	42	20,000	50,000	200,000

2 Techniques Leading to Fixed Target Charm Capabilties

The achievement of million-decay levels is remarkable because, at fixed target experiments, charm is produced only about once in every two hundred photon-induced hadronic interactions and once in every thousand hadron-induced interactions. Furthermore, only about a half percent of the charm decays is reconstructed in these experiments. The search is made even more tedious by the use of more stringent final event selection criteria which further reduces the sample used to obtain the published physics results. The earliest attempts to observe open charm in fixed target experiments failed. The next round of experiments tried to select potential charm events at the time the data were taken using sophisticated trigger processors. More recently, many experiments have turned to simple on-line event selection, leaving sorting through vast amounts of data to later, off-line analysis where sophisticated tracking and vertexing algorithms and final alignment and calibration can be applied.

The cleanliness of the signals comes from the very nature of the fixed target environment. Charm particles are produced moving in the direction of the incident beam. The charm particles live long enough, about 1 picosecond on average, that the location of their disintegration is separated from the point where they were produced - typically a few mm in the laboratory. This separation can be observed, but requires precision measurement of the trajectories of the decay products, with a minimum of material in the way. Depending on the decay mode of the charm particle, cleanliness will be improved by identifying the decay particle types as well. In the e^+e^- machines used to study charm so far, the charm particles are produced at rest, or moving very slowly. Thus, the point of decay usually is indistinguishable from the point of production. This makes it difficult to select only those interactions which contain charm particles, and impossible to examine only those particles in the event coming from a single decay. One must look at all the particles in each event, producing many uninteresting combinations in the search for charm particles.

To illustrate the use of improved technologies in charm experiments, I will cite the series of experiments at Fermilab's Tagged Photon Laboratory. This choice is natural for me since I am most familiar with it. However, the choice is made also because the experiments there have been among the most energetic in applying the new technologies.

The precise trajectory determinations required to provide the reconstructed "event" topologies are made with silicon microstrip detectors (SMDs), first introduced into Fermilab experiments for the 1984-5 fixed target run by Experiment E691.[20] On the left of Fig. 2 is the graphical history of the production and decay of charm particles in one event, reconstructed once the trajectories

Figure 2: On the left, the history of production and decay of charm particles in one event in Fermilab Experiment E691. On the right is the scatter plot, from many such events, of the effective mass of candidate decay particles vs the separation between the production and decay points measured in units of the rms uncertainty in this separation.

of the particles in the event and the particle identities are known. In the event shown, decays of two charm particles are observed and can be projected back to a common production point, also marked by the trajectories of additional particles.

The more certain we are of the existence of the separate decay point and that it is in the anticipated range for typical charm lifetimes, the more certain we can be of having observed a charm particle. This is seen on the right of Figure 2, again from E691. The scatter plot shown there has one dot for each observed candidate decay, plotted (horizontally) at the value of the effective mass of the candidate decay particles and (vertically) at the separation between the production and decay points measured in units of the rms uncertainty in this separation. There is a clear concentration at the effective mass of a D^o meson (1.865 GeV/c^2) with large certainty of production/decay separation. Projecting the events of the scatter plot onto the mass axis leads to the mass distributions seen in Figure 3. The tighter the requirement on separation certainty, the clearer the signal above background. In obtaining final results,

Figure 3: Projections onto the mass axis for increasingly greater certainty of the separation of production and decay points for the events of the scatter plot in Figure 2.

experiments choose their selection criteria such that the error on the physics result is smallest. This is a balance between obtaining the largest number of decay events and the cleanliness of the sample. The cleaner the final sample, the less the contribution to the final error due to estimating the "background".

In additon to silicon microstrip detectors, other new technologies have been required to achieve the improved results. These have included inexpensive magnetic tape storage for large amounts of data, and massive parallel computer systems. Over the last fifteen years, the raw data from fixed target experiments has grown from a few gigabytes to over fifty thousand gigabytes (Table 2). E516, E691 and E769 used open reel magnetic tapes, but E791 was able to take advantage of a new medium, 8 mm video tapes. A single density 8 mm tape can hold the equivalent of thirteen open reel tapes. A typical weekend of data recording in experiment E769 resulted in a forklift worth of tapes. In the next series of fixed target runs, a comparable amount of data was recorded in three hours by E791, and stored in a tray of tapes easily held in one's arms.

The speed of an individual tape writing device for the 8 mm tapes is rather slow. So, the tape writing in E791 was done by an assembly of 42 tape drives writing events out in parallel. The data acquisition architecture supported this parallelism not only in tape writing, but also in the accumulation of data from the front end electronics.

Greater economy in off-line analysis computing was required to handle the massive new data sets. Parallelism was also used to achieve this. It was charm experiment E691 which first used massive parallel-processing computer systems at Fermilab in this way. At that time, home-built, single board computers using commercial CPU chips and home-built control software were used.[21] Later, in time for E769 and other users, commercial workstations were tied together with home-built software.[22]

3 Searches for New Physics: Looking Through the Window

What new measurements do the technologies of the previous section make possible? Among the most interesting measurements with a view towards new physics are the search for violation of the CP symmetry, rare/forbidden decays, and particle-antiparticle mixing.

3.1 CP Violation

The violation of CP symmetry is most notably observed in the macroscopic preponderance of matter over antimatter in the world around us. In the laboratory, microscopic CP violation has only been observed in neutral kaon decay. Although there is a Standard Model explanation for this laboratory violation, the Standard Model cannot explain the origin of the observed matter-antimatter asymmetry around us. Most scientists believe that the Standard Model falls shy by many orders of magnitude. Thus, it is important to look for CP violation outside the Standard Model. Standard Model predictions for the charm system are very small, leaving a window for the discovery of new physics.

To see why the charm sector may be a good place to look, we need to examine the way CP violation might appear. It requires the interference of two amplitudes. One of these amplitudes would be for a Standard Model process. However, the second may be due to a process from new physics. Thus, for example, the appearance of SUSY particles or extra Higgs particles in virtual loops leads to beyond-the-Standard-Model amplitudes.

The largest asymmetries will arise when the interfering weak amplitudes have comparable magnitudes and a large relative phase between them. There is also the need for different strong phases in the final state. Consider a generic pair of such amplitudes for particle decay to a specific final state f:

$$A = A_1 e^{i\delta_1} + A_2 e^{i\delta_2} \tag{1}$$

where δ_i is the strong phase and the amplitudes A_i are the weak decay amplitudes. The CP conjugate amplitude for antiparticle decay to final state $\overline{f}$ is:

$$\overline{A} = \overline{A}_1 e^{i\delta_1} + \overline{A_2} e^{i\delta_2} \tag{2}$$

An asymmetry a results when

$$a = \frac{|A|^2 - |\overline{A}|^2}{|A|^2 + |\overline{A}|^2} = \frac{2|A_1||\overline{A}_2| sin(\theta_1 - \theta_2) sin(\delta_1 - \delta_2)}{|A_1|^2 + |A_2|^2 + 2|A_1||\overline{A_2}| cos(\theta_1 - \theta_2) cos(\delta_1 - \delta_2)} \tag{3}$$

is nonzero. This asymmetry is largest when the two amplitudes are of comparable size, and when ***both*** the strong ***and*** weak phase differences [$(\theta_1 - \theta_2)$ and $(\delta_1 - \delta_2)$, respectively] are large. Charm is specially interesting in that the final state decay particles appear in a region of phase space which has significant resonant structure, leading to large final state phase shifts δ_i. There is also ample evidence that final state interactions are large for D decay. One example is the factor of two difference in the K^+K^- and $\pi^+\pi^-$ decay rates of the neutral D meson. The neutral dikaon decay rate is also very different from the charged dikaon rate. In both cases, the symmetries of weak decay lead to expectations of near equality. Furthermore, the case of singly Cabibbo suppressed decays is particularly relevant since the spectator amplitude provides a size appropriate to creating large asymmetries, even though the overall rate is reduced.

Tables 1 and 3 show the most recent CP violation limits in D decays. There is a window open for non-Standard Model effects. However, we are just now reaching the experimental capability where Cabibbo-suppressed decay modes have sample sizes large enough and with sufficient signal to noise that the constraints will truly limit non-Standard Model possibilities. Furthermore, the open window for new physics here is only a couple of orders of magnitude, making it possible to approach Standard Model effects in a new experiment.

Table 3: Summary of CP violation limits in charged and neutral D decay from Fermilab experiment E791.

Decay Mode	a	90% CL Limits (%)
$D^0 \rightarrow K^- K^+$	-0.010 $\pm$ 0.050	$-9.3 < a < 7.3$
$D^0 \rightarrow \pi^+ \pi^-$	-0.049 $\pm$ 0.084	$-18.6 < a < 8.8$
$D^+ \rightarrow K^- K^+ \pi^+$	-0.014 $\pm$ 0.029	$-6.2 < a < 3.4$
$D^+ \rightarrow \phi \pi^+$	-0.028 $\pm$ 0.036	$-8.7 < a < 3.1$
$D^+ \rightarrow \overline{K}^{*0}(890) K^+$	-0.010 $\pm$ 0.050	$-9.2 < a < 7.2$
$D^+ \rightarrow \pi^- \pi^+ \pi^+$	-0.017 $\pm$ 0.042	$-8.6 < a < 5.2$

3.2 Forbidden Decays

Flavor changing neutral currents are forbidden in the Standard Model at the tree level. Furthermore, higher-order charged-current processes are highly suppressed. Thus, searching for such forbidden decays is another good place to look for physics beyond the Standard Model, especially when the number of decays examined is large.

The best limit so far on such charm decays comes from experiment E771 at Fermilab and WA92 at CERN. Their published 90 % CL limits [7, 8] for $D^0 \rightarrow \mu^+ \mu^-$ are both 4×10^{-6}. While these are significant limits, predictions from Standard Model and non-Standard Model effects both are smaller by a factor of $(M_{\mu^\pm}/M_{D^0})^2$ due to helicity suppression of the decay. Potentially more interesting are the three body decays also listed in Table 1.

We can get some sense of the mass scales being probed in these three body decays by comparing with measured weak decays. Considering the similarity of the tree-level diagrams, we can make comparisons for strange, charm and beauty decays via exchanged neutral vector particles (Fig. 4). Assuming that the matrix elements for the standard W-exchange diagram and H^0-exchange diagram are the same, and that the coupling is the same as the weak coupling, present upper limits from charm reach sensitivities into the hundreds of GeV as listed in Table 4. The calculation is summarized in Eq. 4, where h represents a neutral or charged hadron, M represents matrix elements for the processes of interest, and m represents masses of the exchanged particles in those processes. Similar equations can be written for charged K and B mesons.

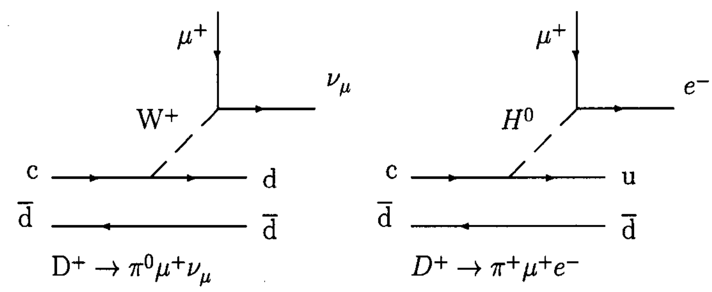

Figure 4: Tree-level diagrams for decays via exchanged neutral vector particles.

$$\frac{\Gamma(D^+ \to h^+\mu^\pm e^\mp)}{\Gamma(D^+ \to h^0\mu^+\nu)} = \frac{\frac{G_F{}^2|M_{H^0}|^2}{m^4_{H^0}}}{\frac{G_F{}^2|M_W|^2}{m^4_W}} = \left[\frac{m_W}{m_{H^0}}\right]^4 \times \frac{|M_{H^0}|^2}{|M_W|^2} \tag{4}$$

3.3 Particle-Antiparticle Mixing

There are opportunities to observe mixing in each of the ground state neutral mesons, from K^0 to D^0 to B^0_d and B^0_s. The charm D^0 is unique among these in that the usual box diagram process (Fig. 5) of the Standard Model gives miniscule predictions for the mixing rate. Due to the fact that the very massive top quark does not participate in the loop, the CKM elements are small, and the GIM mechanism [23] cancelation is effective. Thus, the Standard Model predictions are at the 10^{-8} to the 10^{-10} level.[17] Even long range effects are now thought to be small.[26]

Fortunately, the experimental situation is also propitious. We use the D^{*+} and D^{*-} with their respective decays to $D^0\pi^+$ and $\overline{D}^0\pi^-$ to obtain a well-understood sample of produced D^0 and $\overline{D}^0$. The sign of the decay π identifies the particle/antiparticle nature of the D at birth. The particle/antiparticle nature of the D at its decay is determined by the sign of its decay kaons and leptons. In fixed-target experiments, the proper lifetime is obtained from the separation of the production and decay points and the measured momentum of the D. Thus, we can follow any mixing induced particle/antiparticle oscillation as a function of proper time.

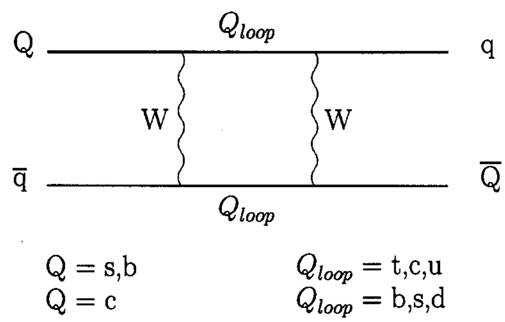

Figure 5: Box diagram for particle-antiparticle mixing in the Standard Model.

Table 4: Mass scales probed in searches for lepton number violation.

Decay Mode	90% CL Limit	Implied Mass Limit
$K^+ \to \pi^+\mu^+e^-$	2×10^{-10}	$M_{H^0} > 9$ TeV
$K^+ \to \pi^+\mu^-e^+$	7×10^{-9}	$M_{H^0} > 4$ TeV
$D^+ \to \pi^+\mu^\pm e^\mp$	1×10^{-4}	$M_{H^0} > 410$ GeV
$D^+ \to K^+\mu^\pm e^\mp$	1×10^{-4}	$M_{H^0} > 220$ GeV
$B^+ \to \pi^+\mu^\pm e^\mp$	6×10^{-3}	Need $\Gamma(B \to h\mu\nu)$
$B^+ \to K^+\mu^\pm e^\mp$	6×10^{-3}	Need $\Gamma(B \to h\mu\nu)$

This last capability is especially important in the case of hadronic decays of the $D^0/\overline{D}^0$. A mixing signal can be masked by production of the same final state via doubly-Cabibbo-suppressed (DCS) decay. However, DCS decays have a simple exponential decay probability while a pure mixing signal will grow with time for short times. The rate for a pure mixing signal is proportional to the product of the square of the proper time and an exponential, since it takes time for a D^0 to turn into a $\overline{D}^0$. There is also the possibility that the mixing and DCS amplitudes will interfere, giving a term in the rate proportional to the product of proper time and an exponential.[24] The final result requires a likelihood fit over the observed D^0 mass, observed D^{*0} minus D^0 mass difference and proper decay time. Depending on how general one allows the model of CP violation to be, uncertainties can vary by factors of three, with corresponding variations in the upper limits reported.[16] For semileptonic decays, the situation is simpler. There is no doubly-Cabibbo-suppressed decay to confuse measurements. The upper limits now available are of the same order as those from hadronic decays. [18] Again, a large window is open for new physics discovery in charm decay.

4 Prospects and Conclusions

Given the remaining windows for new physics in charm, what is possible? Have the present technologies run their course for fixed target charm? The CERN COMPASS fixed target experiment is pushing ahead in an external beam line. Another possibility is that the HERA-B fixed target experiment using internal wire targets in the HERA circulating proton beam will push yet further with charm. However, the focus on B physics leads to active attempts to avoid charm event data. Will enough charm sneak through the event selection to push the charm frontier? The e^+e^- B Factories also will be copious sources of charm data. Will they catch and surpass the fixed target lead? The asymmetric e^+e^- machines will have some of the same long-flight-path advantages of the fixed target environment. Here in China, active plans for a Tau-Charm Factory remain uncertain.

The most promising combination of production rate and long-flight-path comes from hadron collider experiments (BTeV at Fermilab and LHC-B at CERN). These experiments, while focused on B physics, also are being thought about now for charm. I am happy to note here in China that research groups from Nanjing University (T.Y. Chen), Shandong University (M. He), and the China University of Science and Technology in Hefei (X.Q. Yu) are participating in the BTeV effort. Such a collider-charm direction might provide a new chapter for charm, and continue the twenty-year exponential growth in useful charm decays observed. Such improvement will be necessary to make a significant step in charm physics. It may be that just such a step will provide a discovery explaining parts of our world we cannot now understand. It would be nice to know what happened to all the antimatter in the universe, for example. And, why are there three generations of quark pairs?

5 Acknowledgments

I am happy to acknowledge my colleagues, especially those on the series of Fermilab charm experiments at the Tagged Photon Laboratory (E516, E691, E769 and E791) and on the BTeV proposal. The insights summarized here have come from fruitful collaboration with them. I also thank Dan Kaplan for use of an original version of Table 1, which was modified for this talk, and David Christian, David Johnson and Jean Slaughter for help with the figures.

This work is supported by the United States Department of Energy through Fermilab, which is operated by Universities Research Association Inc. under Contract No. DE-AC02-76CH03000.

References

1. CLEO Collaboration, J. Bartelt *et al.*, Phys. Rev. D **52**, 4860, (1995).
2. E791 Collaboration, E.M. Aitala *et al.*, Accepted for publication in Phys. Lett. B, hep-ex/9711003.
3. E791 Collaboration, E.M. Aitala *et al.*, Phys. Lett. B **403**, 377 (1997).
4. E687 Collaboration, P.L. Frabetti *et al.*, Phys. Rev. D **50**, R2953 (1994).
5. F. Buccella *et al.*, Phys. Lett. B **302**, 319 (1993);
   A. Pugliese and P. Santorelli, "Two Body Decays of D Mesons and CP Violating Asymmetries in Charged D Meson Decays," *Proc. Third Workshop on the Tau/Charm Factory*, Marbella, Spain, 1–6 June 1993, Edition Frontieres (1994), p. 387.
6. Z. Xing, Phys. Lett. B **353**, 313 (1995).
7. E771 Collaboration, T. Alexopoulos *et al.*, Phys. Rev. Lett. **77**, 2380 (1996).
8. WA92 Collaboration, M. Adamovich *et al.*, Phys. Lett. B **408**, 469 (1997).
9. J. L. Hewett, "Searching for New Physics with Charm," SLAC-PUB-95-6821, hep-ph/9505246, to appear in *Proc. LISHEP95 Workshop*, Rio de Janeiro, Brazil, Feb. 20–22, 1995.
10. E653 Collaboration, K. Kodama *et al.*, Phys. Lett. B **345**, 85 (1995).
11. P.D. Sheldon, "Searching for CP Violation, Flavor Changing Neutral Currents, and Lepton Number Violation in Charm Decay," in **The Fu-**

ture of High-Sensitivity Charm Experiments, *Proc. CHARM2000 Workshop*, Fermilab, June 7–9, 1994, D. Kaplan and S. Kwan, *eds.*, FERMILAB-Conf-94/190, p. 25.
12. E791 Collaboration, E.M. Aitala *et al.*, Phys. Rev. Lett. **76**, 364 (1996).
13. E687 Collaboration, P.L. Frabetti *et al.*, Phys. Lett. B **398**, 239 (1997).
14. R.M. Barnett *et al.* (Particle Data Group), Phys. Rev. D **54**, 1 (1996).
15. E691 Collaboration, J. C. Anjos *et al.*, Phys. Rev. Lett. **60**, 1239 (1988); See also Reference [16].
16. E791 Collaboration, E.M. Aitala *et al.*, Phys. Rev. D **57**, 13 (1998).
17. G. Burdman, "Charm Mixing and *CP* Violation in the Standard Model," in **The Future of High-Sensitivity Charm Experiments**, *op. cit.* p. 75, and "Potential for Discoveries in Charm Meson Physics," in **Workshop on the Tau/Charm Factory**, J. Repond, *ed.*, Argonne National Laboratory, June 21–23, 1995, AIP Conference Proceedings No. 349 (1996), p. 409.
18. E791 Collaboration, E.M. Aitala *et al.*, Phys. Rev. Lett. **77**, 2384 (1996).
19. Y. Nir, "Exploring New Physics with CP Violation in Neutral D and B Decays," WIS-95-28-PH, hep-ph/9507290, presented at the *6th International Symposium on Heavy Flavor Physics*, Pisa, Italy, 6–9 June 1995.
20. The previous most successful use of SMDs in high energy physics experiments was by the NA11 collaboration at CERN, who did so much to develop these devices. B. Hyams *et al.*, Nucl. Inst. and Meth., **205**, 99 (1983). J. Kemmer, Nucl. Inst. and Meth., **169**, 499 (1980).
21. J. Biel *et al.*, Proc. Int. Conf. Computing in High Energy Physics, Asilomar, Feb. 2-6, 1987, Computer Physics Communications, **45**, 331 (1987).
22. C. Stoughton and D.J. Summers, Computers in Physics, **6**, 371 (1992); F. Rinaldo and S. Wolbers, Computers in Physics, **7**, 184 (1993); S. Bracker *et al.*, IEEE Trans. on Nucl. Sci., **43**, 2457 (1996).
23. S. L. Glashow, J. Iliopoulos, and L. Maiani, Phys. Rev. D **2**, 1285 (1970); S. L. Glashow and S. Weinberg, Phys. Rev. D **15**, 1958 (1977); E. A. Paschos, Phys. Rev. D **15**, 1966 (1977).
24. G. Blaylock, A. Seiden, and Y. Nir, Phys. Lett. B **355**, 555 (1995).
25. WA92 Collaboration, M. Adamovich *et al.*, Phys. Lett. B **353**, 563 (1995).
26. J. F. Donoghue *et al.*, Phys. Rev. D **33**, 179 (1986); H. Georgi, Phys. Lett. B **297**, 353 (1992); and T. Ohl, G. Ricciardi, and E. H. Simmons, Nucl. Phys. **B403**, 605 (1993). L. Wolfenstein, Phys. Lett. **164B**, 170 (1985).

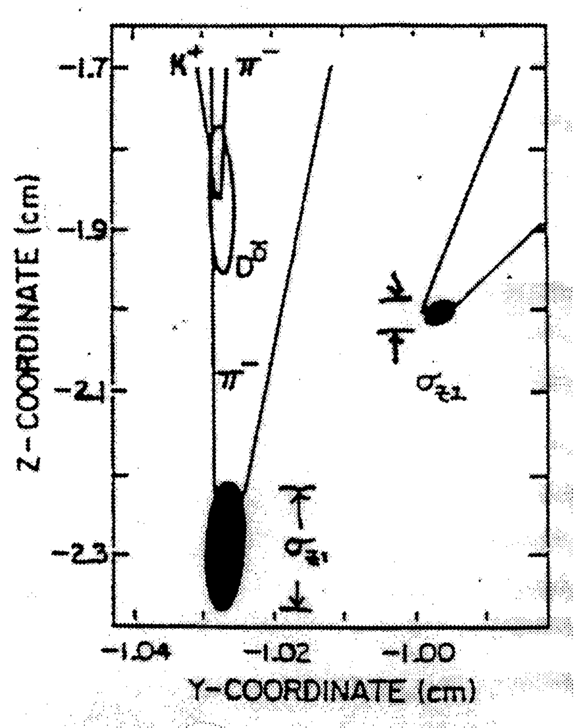

K+
π−
D0
π−
σz1
σz2
-1.7
-1.9
-2.1
-2.3
-1.04
-1.02
-1.00
Z-COORDINATE (cm)
Y-COORDINATE (cm)

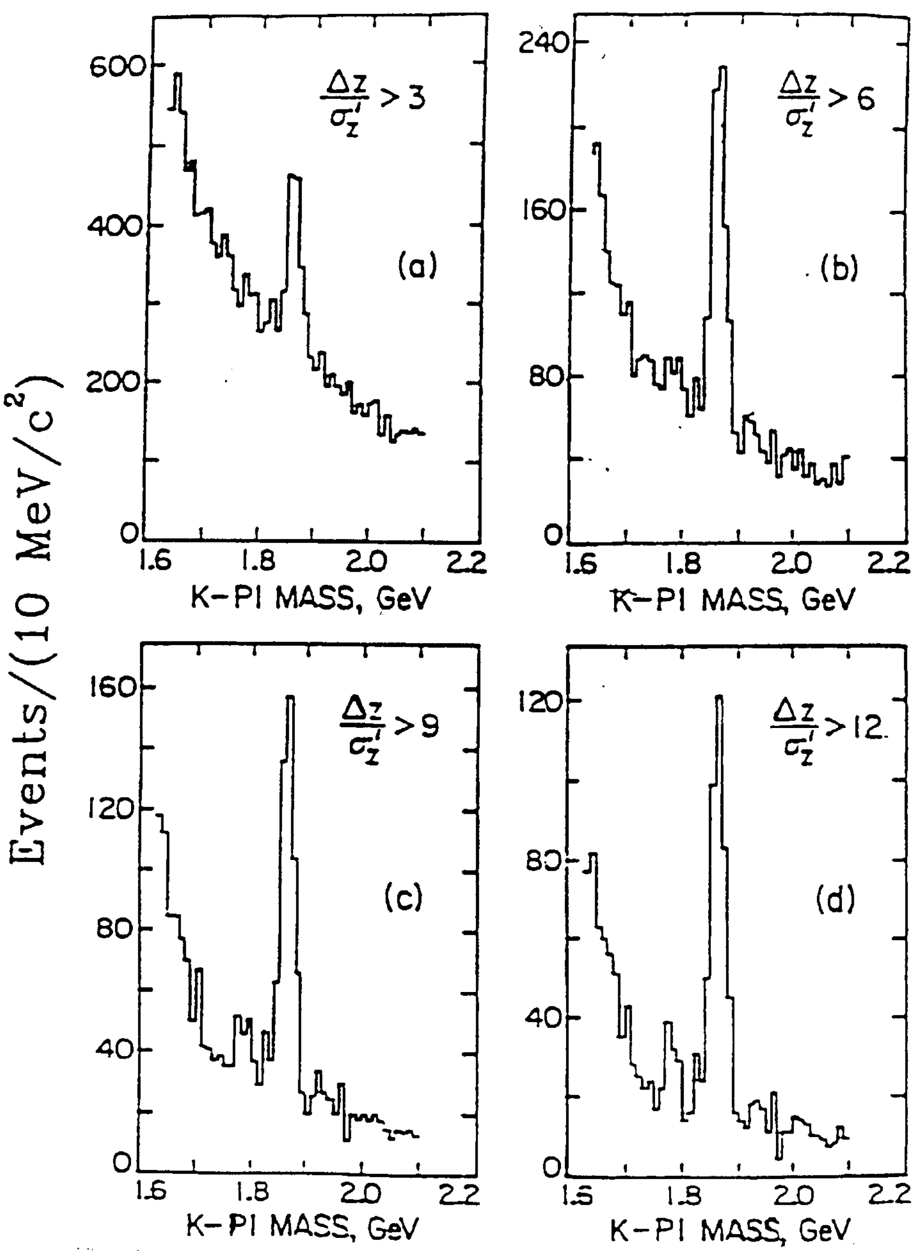

Events/(10 MeV/c^2)
$\frac{\Delta z}{\sigma_z'} > 3$
(a)
600
400
200
0
1.6
1.8
2.0
2.2
K-PI MASS, GeV
$\frac{\Delta z}{\sigma_z'} > 6$
(b)
240
160
80
0
1.6
1.8
2.0
2.2
K-PI MASS, GeV
$\frac{\Delta z}{\sigma_z'} > 9$
(c)
160
120
80
40
0
1.6
1.8
2.0
2.2
K-PI MASS, GeV
$\frac{\Delta z}{\sigma_z'} > 12$
(d)
120
80
40
0
1.5
1.8
2.0
2.2
K-PI MASS, GeV

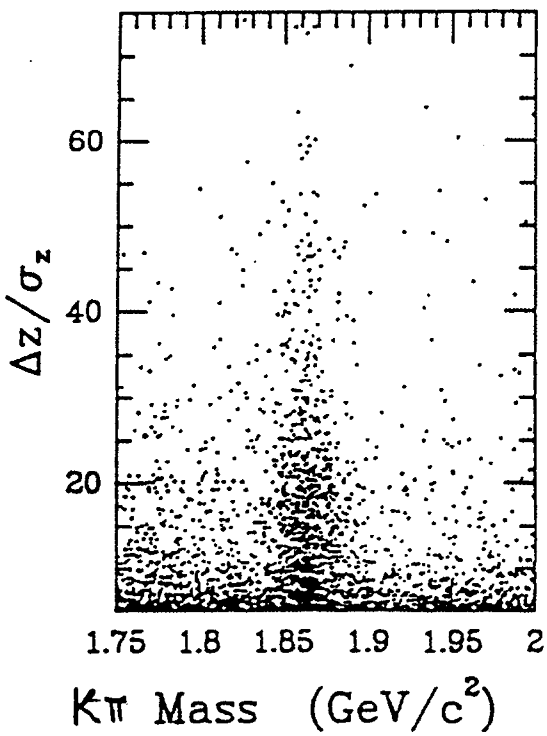
60
40
20
Δz/σ_z
1.75 1.8 1.85 1.9 1.95 2
Kπ Mass (GeV/c²)